

all effective inhibitors of the β -glucuronidase enzyme in vitro (with K_i values of 160, 210, 680, and 1400 nM, respectively), and they maintain potent efficacy in living bacterial cells (EC_{50} values of 18, 28, 230, and 1300 nM, respectively) (Table 1) without affecting bacterial cell growth or survival under aerobic or anaerobic conditions (figs. S16 and S17) or killing mammalian epithelial cells (fig. S18). Lower EC_{50} values relative to the K_i values likely reflect relatively low β -glucuronidase concentrations in cells. Key residues of the “bacterial loop” identified in the *E. coli* β -glucuronidase crystal structure are present in 98% of the β -glucuronidases sequenced from human GI bacteria, and 91% of those sequences contain residues that appear capable of forming inhibitor contacts (figs. S13 and S14). Disruption of β -glucuronidase activity is also demonstrated in bacterial species beyond *E. coli* (Fig. 3D). Taken together, the data presented here strongly support the hypothesis that microbial β -glucuronidases can be inhibited to prevent the GI production of toxic CPT-11 metabolites. However, full pharmacokinetic studies demonstrating, for example, a reduction in GI SN-38G levels or improved CPT-11 efficacy will be required to unambiguously prove this hypothesis. In addition, the breadth of inhibitor efficacy on human GI bacteria requires further assessment. Still, these initial results involving the oral dosing of an unmodified lead compound are highly promising. If successfully translated to humans, leads like those described here could allow dose intensification of CPT-11, enabling studies of whether efficacy could be improved in relevant human cancers by reducing one of the current dose-limiting side effects. The strategy of selective targeting of an enzyme present in bacterial symbiotes to address a specific clinical problem could po-

tentially be applied more broadly as we deepen our understanding of the essential and dynamic roles that commensal bacteria play in promoting human health.

References and Notes

1. Y. H. Hsiang, R. Hertzberg, S. Hecht, L. F. Liu, *J. Biol. Chem.* **260**, 14873 (1985).
2. M. R. Redinbo, J. J. Champoux, W. G. Hol, *Curr. Opin. Struct. Biol.* **9**, 29 (1999).
3. J. F. Pizzolato, L. B. Saltz, *Lancet* **361**, 2235 (2003).
4. Y. Pommier, *Nat. Rev. Cancer* **6**, 789 (2006).
5. N. F. Smith, W. D. Figg, A. Sparreboom, *Toxicol. In Vitro* **20**, 163 (2006).
6. R. H. J. Mathijssen *et al.*, *Clin. Cancer Res.* **7**, 2182 (2001).
7. M. K. Ma, H. L. McLeod, *Curr. Med. Chem.* **10**, 41 (2003).
8. S. Nagar, R. L. Blanchard, *Drug Metab. Rev.* **38**, 393 (2006).
9. P. J. Tobin, H. M. Dodds, S. Clarke, M. Schnitzler, L. P. Rivory, *Oncol. Rep.* **10**, 1977 (2003).
10. A. Stein, W. Voigt, K. Jordan, *Ther. Adv. Med. Oncol.* **2**, 51 (2010).
11. A. Kurita *et al.*, *Cancer Chemother. Pharmacol.* 10.1007/s00280-010-1310-4 (2010).
12. Z. P. Hu *et al.*, *Toxicol. Appl. Pharmacol.* **216**, 225 (2006).
13. See supporting material on Science Online.
14. D. Flieger *et al.*, *Oncology* **72**, 10 (2007).
15. J. H. Cummings, G. T. Macfarlane, *J. Parenter. Enteral Nutr.* **21**, 357 (1997).
16. F. Guarner, J. R. Malagelada, *Lancet* **361**, 512 (2003).
17. S. B. Levy, B. Marshall, *Nat. Med.* **10** (suppl.), S122 (2004).
18. C. E. Nord, L. Kager, A. Heimdahl, *Am. J. Med.* **76**, 99 (1984).
19. C. D. Settle, M. H. Wilcox, *Aliment. Pharmacol. Ther.* **10**, 835 (1996).
20. S. Sears, P. McNally, M. S. Bachinski, R. Avery, *Gastrointest. Endosc.* **50**, 841 (1999).
21. D. Stamp, *Med. Hypotheses* **63**, 555 (2004).
22. L. Yang, Z. Pei, *World J. Gastroenterol.* **12**, 6741 (2006).
23. S. H. Cohen *et al.*, *Infect. Control Hosp. Epidemiol.* **31**, 431 (2010).
24. A. Basińska, B. Floriańczyk, *Ann. Univ. Mariae Curie Skłodowska Med.* **58**, 386 (2003).
25. A. H. Farnleitner, L. Hocke, C. Beiwil, G. G. Kavka, R. L. Mach, *Water Res.* **36**, 975 (2002).
26. S. Jain *et al.*, *Nat. Struct. Biol.* **3**, 375 (1996).
27. M. Fittkau, W. Voigt, H.-J. Holzhausen, H. J. Schmoll, *J. Cancer Res. Clin. Oncol.* **130**, 388 (2004).
28. W. M. Russell, T. R. Klaenhammer, *Appl. Environ. Microbiol.* **67**, 1253 (2001).
29. T. Niwa, T. Tsuruoka, S. Inoue, Y. Naito, T. Koeda, *J. Biochem.* **72**, 207 (1972).
30. S. Jain *et al.*, *Nat. Struct. Mol. Biol.* **3**, 375 (1996).
31. R. H. Jacobson, X. J. Zhang, R. F. DuBose, B. W. Matthews, *Nature* **369**, 761 (1994).
32. A. Marchler-Bauer *et al.*, *Nucleic Acids Res.* **37** (database issue), D205 (2009).
33. J. H. Zhang, T. D. Chung, K. R. Oldenburg, *J. Biomol. Screen.* **4**, 67 (1999).
34. J. Ray, V. Scarpino, C. Laing, M. E. Haskins, *J. Hered.* **90**, 119 (1999).
35. P. J. Turnbaugh *et al.*, *Nature* **449**, 804 (2007).
36. C. L. Sears, *Anaerobe* **11**, 247 (2005).
37. J. P. Grill, C. Manginot-Dürri, F. Schneider, J. Ballongue, *Curr. Microbiol.* **31**, 23 (1995).
38. M. G. Brattain, W. D. Fine, F. M. Khaled, J. Thompson, D. E. Brattain, *Cancer Res.* **41**, 1751 (1981).
39. B. Siegmund *et al.*, *J. Pharmacol. Exp. Ther.* **296**, 99 (2001).
40. We thank members of the Redinbo Laboratory at UNC Chapel Hill, the Mani lab and Einstein College of Medicine, and the BRITE Institute for experimental assistance and helpful discussions; B. Allard at UNC Chapel Hill for her expert help with the cytotoxicity assay; B. Sartor at UNC for providing bacterial cell lines; and E. Burgos in the Schramm lab at Einstein for use of the HPLC. Supported by NIH grant CA98468 (M.R.R.), the SPIRE Postdoctoral Fellowship Program at UNC Chapel Hill (K.T.L.), Damon Runyon Cancer Research Foundation grant C15-02 and NIH grant CA127231 (S.M.), and a grant from the Golden Leaf Foundation and the State of North Carolina (L.-A.Y.). Atomic coordinates and structure factors have been deposited with the PDB (accession codes: 3K4A, 3K46, 3K4D, 3LPF, and 3LPG). The authors remember Lisa Benkowski and Stacey Micoli, for whom CPT-11's efficacy was limited by its toxicity.

Supporting Online Material

www.sciencemag.org/cgi/content/full/330/6005/831/DC1
Materials and Methods
SOM Text
Figs. S1 to S19
Tables S1 and S2
References

20 April 2010; accepted 27 August 2010
10.1126/science.1191175

The Mechanism for Activation of GTP Hydrolysis on the Ribosome

Rebecca M. Voorhees,* T. Martin Schmeing,*‡ Ann C. Kelley, V. Ramakrishnan†

Protein synthesis requires several guanosine triphosphatase (GTPase) factors, including elongation factor Tu (EF-Tu), which delivers aminoacyl-transfer RNAs (tRNAs) to the ribosome. To understand how the ribosome triggers GTP hydrolysis in translational GTPases, we have determined the crystal structure of EF-Tu and aminoacyl-tRNA bound to the ribosome with a GTP analog, to 3.2 angstrom resolution. EF-Tu is in its active conformation, the switch I loop is ordered, and the catalytic histidine is coordinating the nucleophilic water in position for inline attack on the γ -phosphate of GTP. This activated conformation is due to a critical and conserved interaction of the histidine with A2662 of the sarcin-ricin loop of the 23S ribosomal RNA. The structure suggests a universal mechanism for GTPase activation and hydrolysis in translational GTPases on the ribosome.

In all stages of protein synthesis the ribosome requires exogenous protein factors, including several guanosine 5'-triphosphate (GTP)-hydrolyzing enzymes known as GTPases. These proteins are essential and highly conserved and include elongation factor Tu (EF-Tu), which de-

livers aminoacyl-tRNA to the ribosome as part of a ternary complex (TC) with GTP, as well as elongation factor G and initiation factor 2 (I). The architecture of the GTP-binding domain is similar in all translational GTPases from bacteria to higher eukaryotes, and hydrolysis is accom-

panied by conformational changes in the conserved switch I and II regions (2). Furthermore, translational GTPases bind to the same region of the ribosome in all species (3, 4). The conserved binding site and structural similarities suggest that there is a common mechanism by which the ribosome activates GTP hydrolysis in these factors. However, despite more than 40 years of research, this mechanism has remained elusive.

The catalysis of GTP hydrolysis in translational GTPases requires an invariant histidine (His⁸⁴ in EF-Tu) that acts as a general base, abstracting a proton from a water molecule, for inline attack on the γ -phosphate of GTP (5–7). The intrinsic GTPase activity of translational GTPases

MRC Laboratory of Molecular Biology, Cambridge CB2 0QH, UK.

*These authors contributed equally to this work.

†To whom correspondence should be addressed. E-mail: ramak@mrc-lmb.cam.ac.uk

‡Present address: Biochemistry Department, McGill University, Bellini Life Sciences Complex Room 465, 3649 Promenade Sir William Osler, Montreal, Quebec H3G 0B1, Canada. E-mail: martin.schmeing@mcgill.ca

is low (8) and increases markedly upon productive binding to the ribosome (9, 10). For EF-Tu, efficient GTPase activation requires the binding of an aminoacyl-tRNA to its cognate mRNA codon. Activation could be accomplished either indirectly, i.e., proper ribosome binding induces an active conformation of the G factor, and/or more directly, with the ribosome playing an active role in catalysis. The ribosomal components that compose the GTPase binding site and therefore may be important for hydrolysis include the sarcin-ricin loop (SRL) of the 23S ribosomal RNA (rRNA) (3, 11), the L11 protein and rRNA (12), and the protein L12 (13).

Premature GTP hydrolysis in EF-Tu is thought to be prevented by a “hydrophobic gate,” consisting of residues Val²⁰ of the P loop and Ile⁶⁰ of switch I, which restricts access of His⁸⁴ to the catalytic water (6). Proposals of how the hydrophobic gate is “opened” include that His⁸⁴ would simply “push” through the gate when ac-

tivated (6), or that a disordering (14, 15) or radical rearrangement of switch I removes this steric block (16–18). However, these hypotheses were made on the basis of structures of EF-Tu in isolation, or studies of the posthydrolysis, kirromycin-stalled complex on the ribosome. A conclusive understanding of how GTPase activation occurs on the ribosome requires the structure of a complex of EF-Tu before GTP hydrolysis.

Here, we report the crystal structure of EF-Tu bound to the 70S ribosome along with Trp-tRNA^{Trp}, and the antibiotic paromomycin, stalled in the activated conformation by the GTP analog β - γ -methylene-guanosine 5'-triphosphate (GDPCP), at 3.2 Å resolution. The structure reveals the GTPase-competent form of EF-Tu and suggests a universal mechanism for GTP hydrolysis on the ribosome.

The overall conformations of the ribosome, EF-Tu, and the aminoacyl-tRNA are as previously reported (15) (Fig. 1A), and all the conformational changes predicted to communicate codon recog-

nition to EF-Tu are observed, except that the switch I loop is ordered in the GTPase center (Fig. 1B). Additionally, the catalytic histidine is activated and coordinating a water for inline attack on the γ -phosphate of the GTP analog (Fig. 1C).

As well as providing insight into the mechanism of GTP hydrolysis of all translational GTPases, this structure represents a key, missing state in the decoding pathway. High-resolution crystal structures have previously been determined for the isolated TC (19) and the posthydrolysis state stalled on the ribosome by kirromycin (15). In conjunction with these two structures, this structure of the activated GTP state bound to the ribosome provides insight into the chemical details of the complete hydrolysis pathway of EF-Tu.

Before ribosome binding, the TC contains an unbound tRNA, and switch I, switch II, and the P loop are ordered around the GTP molecule in the active site. However, the catalytic His⁸⁴ (switch II) is rotated away from GTP in an inactive con-

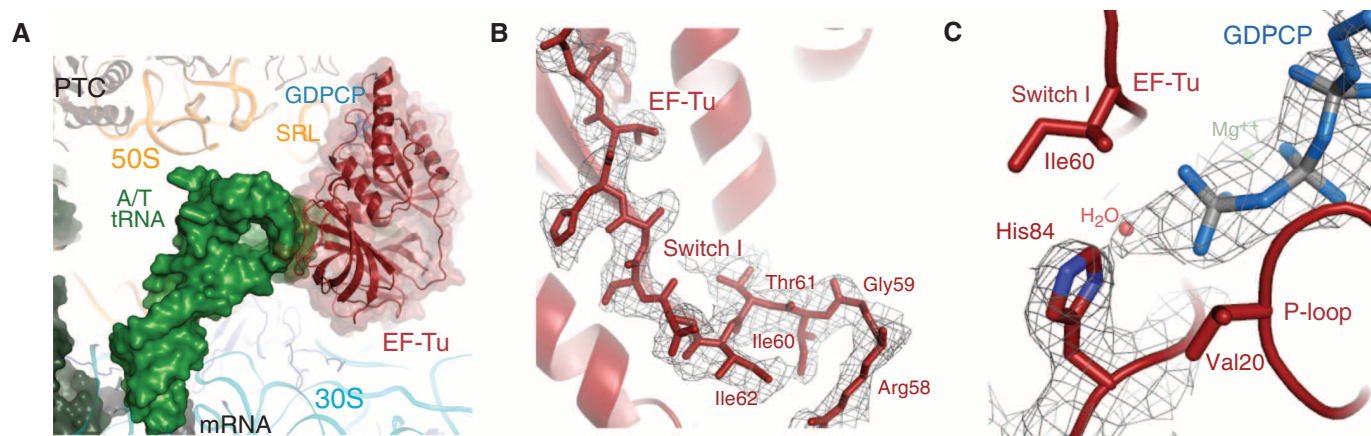


Fig. 1. The ternary complex bound to the ribosome in the activated state. (A) EF-Tu (red) and aminoacyl-tRNA (green) bound to the 70S ribosome, stabilized by GDPCP (blue). (B) Unbiased $F_o - F_c$ electron density displayed for the switch I loop. (C) Unbiased $F_o - F_c$ electron density for GDPCP, the water molecule (red sphere), and His⁸⁴ positioned in a catalytically active conformation. *E. coli* number is used throughout the text.

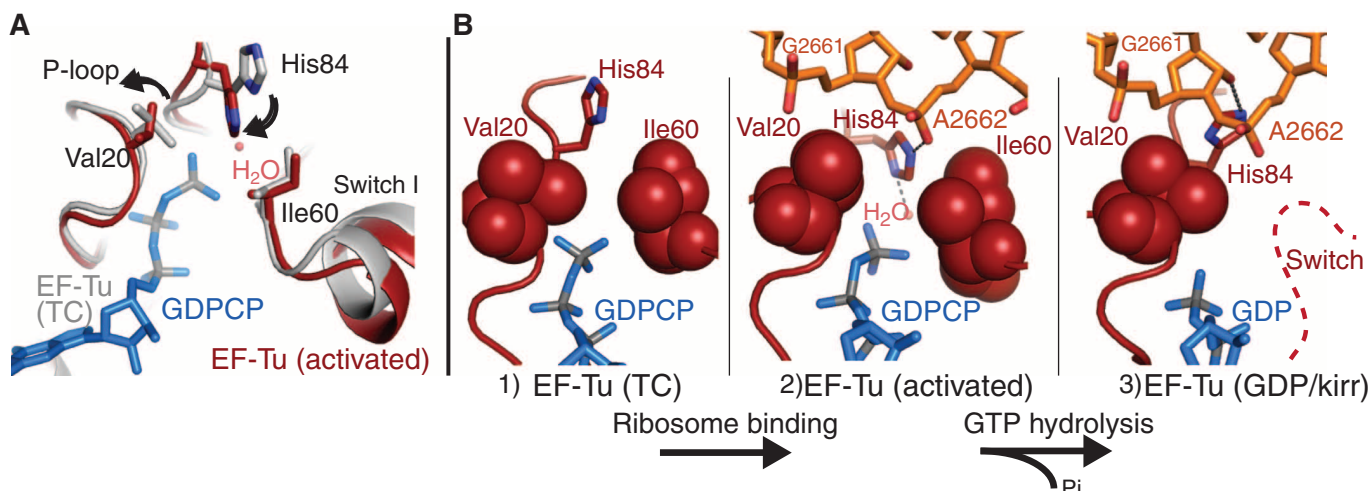


Fig. 2. The active site of EF-Tu during decoding. (A) Superposition of the GTPase centers from the isolated TC (gray) (19) and the TC-GDPCP-ribosome (red). Small movements are observed for hydrophobic gate residues Val²⁰ and Ile⁶⁰. (B) GTPase activation allows the phosphate of A2662 of the SRL (orange) to position His⁸⁴ into the active site. After GTP hydrolysis (15) and P_i release, switch I becomes disordered (dashed line) and His⁸⁴ rotates away from GDP.

formation (19). Ribosome binding and codon recognition induce the bent tRNA in the A/T state (where the anticodon interacts with the mRNA in the A site and the acceptor end is bound to EF-Tu) (20), as well as conformational changes in the tRNA, 30S ribosomal subunit, and EF-Tu essential for triggering GTP hydrolysis (15). Productive binding of the TC to the ribosome results in a shift of the G domain of EF-Tu by up to ~ 7 Å, to avoid a steric clash between switch I and the SRL of the 23S rRNA. Ribosome binding also causes a distortion in the 3' end of the aminoacyl-tRNA between residues 72 and 75 as reported (15), which releases contacts between the tRNA backbone and the switch I loop (fig. S1). However, in contrast to our previous prediction, this alone does not disorder switch I, which is largely unchanged from its conformation in the isolated TC (Fig. 2A) (19).

Although switch I remains ordered in the active site, the catalytic histidine is in its activated conformation (Fig. 2). We see no evidence that large rearrangements are required for catalysis (fig. S1) (15–18). Instead, the “open” state is reached by a 1.2 Å shift in the side chain of Ile⁶⁰, an $\sim 80^\circ$ rotation of the side chain of Val²⁰, and a small movement of the backbone of residues 19 to 22 away from the GTP analog (Fig. 2). The conformation of switch I is similar to that modeled for the eukaryotic ortholog of EF-G bound to β - γ -imidoguanosine 5'-triphosphate (GDPNP) on the ribosome (21).

These small changes in the active site would subtly increase the space between switch I and the P loop, possibly facilitating GTP hydrolysis. However, our analysis suggests that even the “closed” hydrophobic gate (19) could accommodate the activated conformation of His⁸⁴ and would not preclude binding of a water in its catalytic

position, though a water is not observed. Instead, to prevent GTP hydrolysis before codon recognition, the activated conformation of His⁸⁴ must be unfavorable in solution. Indeed, the adjacent residues, Gly⁸³ and Pro⁸², are more than 98% conserved, and mutational data suggest that the flexibility of these residues may be important (19, 22).

GTPase activation by the ribosome therefore does not involve an opening of the hydrophobic gate, but rather requires the specific positioning of His⁸⁴ into the active site. In this activated structure of EF-Tu, the phosphate of residue A2662 of the SRL orders His⁸⁴ in its catalytic conformation, which then acts as a general base to allow the nucleophilic water molecule to attack the γ -phosphate of GTP (Figs. 2 and 3). When positioning His⁸⁴, the phosphate of A2662 could also conceivably participate in a charge-relay system that facilitates the deprotonation of the water by His⁸⁴, playing a role analogous to that of the catalytic aspartic acid in serine proteases (23). However, the existence and contribution of such a mechanism would need to be assessed by biochemical experiments. The activation does not require movements within the SRL, as its overall conformation is similar to that in previous 70S ribosome structures (15, 24). This critical role of the sarcin-ricin loop answers the long-standing question of why the SRL is important for binding and GTPase activation by the ribosome. The toxin α -sarcin acts by cleaving the 23S rRNA between residues G2661 and A2662 (11), exactly the phosphate group activating His⁸⁴. It is therefore clear why cleaving this bond, or introducing mutations at nearby sites in the SRL (25), leads to defects in His⁸⁴ positioning and GTP hydrolysis (11, 26). α -Sarcin is active against both bacterial and eukaryotic ribosomes and causes similar defects in the function of their respective

translational GTPases (11, 26). We therefore predict that the positioning of the catalytic histidine into the active site by A2662 of the SRL is the universal mechanism for GTPase activation on the ribosome. EF-G has additional interactions between its domain 3 and A2660 of the SRL, which explains why depurination of A2660 by the toxin ricin affects EF-G, but not EF-Tu (26).

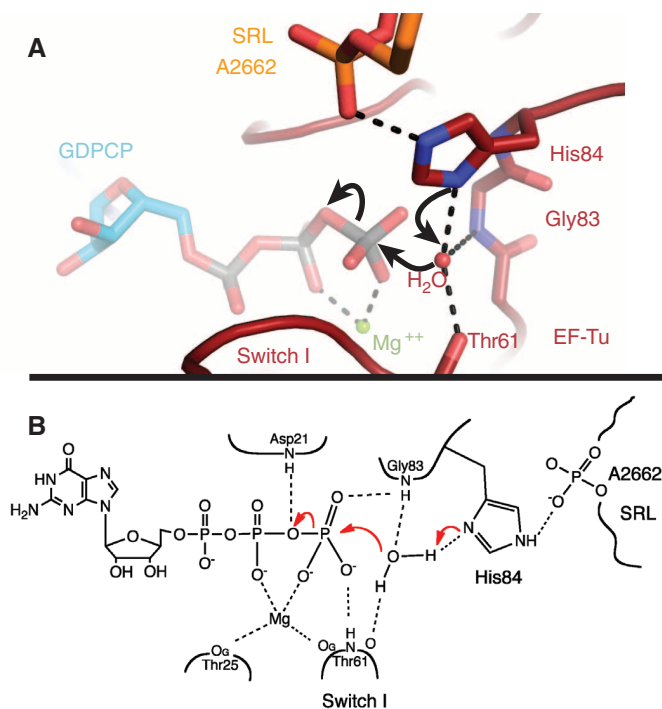
Ribosome association alone is not sufficient for A2662 to activate His⁸⁴. Rather, all of the conformational changes that occur upon cognate codon recognition in the ribosome (codon-anticodon monitoring, domain closure), the tRNA (A/T state, 3' end distortion), and EF-Tu (β -loop interaction with 30S shoulder, G domain shift) (15) are essential for properly positioning the GTPase center of EF-Tu for activation by the SRL. The energy required to induce these movements is balanced against the energy derived from binding of a cognate tRNA, including that from interactions of the 16S rRNA residues A1492, A1493, and G530 with the minor groove of the codon-anticodon helix (27). Even subtle changes in the position of the G domain relative to the SRL would cause defects in GTPase activation by preventing A2662 from properly placing His⁸⁴ into the active site.

The activation of GTP hydrolysis in EF-Tu by the SRL is similar to the regulation of cellular GTPases by their partner proteins. Unlike the classic cases of Rho and Ras, in which their GTPase activator proteins (GAPs) directly donate catalytic residues (28, 29), other G proteins are activated by “regulator of G-protein signaling” (RGS) proteins, which instead stabilize the active conformation of the GTPase (30). By analogy, the SRL acts as an RGS-type GAP for translational GTPases.

All components required for GTPase activation should be present in this catalytically active structure. Notably, we see no evidence that ribosomal protein L12, predicted to be important for hydrolysis, is interacting with EF-Tu, though such an interaction would be compatible with the crystal packing. Indeed, it is sterically impossible for L12 or any other protein to interact with GTP, consistent with data suggesting that L12 does not function directly in catalysis (13, 31, 32). Furthermore, deletion of the eukaryotic orthologs of L12 from yeast ribosomes is not lethal (33), indicating that L12 may not be critical for achieving GTP hydrolysis.

Following hydrolysis, inorganic phosphate (P_i) is released from EF-Tu. The γ -phosphate of GTP makes several contacts with switch I through residue Thr⁶² (Fig. 3 and fig. S3), and release of P_i could destabilize and perhaps even require movement of switch I. This and the loss of interactions with the 3' end of the tRNA backbone (fig. S1) lead to the previously observed disordering of switch I (15, 18). Furthermore, comparison of the kirromycin- and the GDPNP-stalled complexes shows a rotation of $\sim 4^\circ$ of the G domain relative to domains 2 and 3 (fig. S4). There is a corresponding movement in the acceptor stem of the tRNA, in order to maintain interactions with switch II (15), which could explain the subtle

Fig. 3. Chemical mechanism of GTP hydrolysis. **(A)** Highly conserved His⁸⁴ acts as a general base to activate the catalytic water molecule, which is positioned by interactions with Thr⁶¹, Gly⁸³, and His⁸⁴. **(B)** Chemical structure diagram depicting the interactions between EF-Tu and GTP that stabilize the β and γ phosphates, allowing GTP hydrolysis to occur (see also fig. S3).



difference in fluorescence signal between the activated and kirromycin-stalled states (34).

This structure of 70S-tRNA-EF-Tu-GDPCP provides an atomic-resolution model of a translational GTPase in its activated state. Codon recognition leads to a series of conformational changes in the 30S subunit, tRNA, and EF-Tu that position EF-Tu for GTP hydrolysis. GTPase activation does not require a large opening of the “hydrophobic gate,” but instead requires the positioning of the catalytic histidine into the active site by the SRL residue A2662. The high level of sequence and structural conservation between all translational GTPases suggests that although each factor recognizes a distinct ribosomal state, each must bind in such a way that the SRL interacts with its catalytic histidine. Therefore, GTPase activation by the SRL is the universal mechanism for triggering GTP hydrolysis on the ribosome across all kingdoms of life.

References and Notes

1. T. Margus, M. Remm, T. Tenson, *BMC Genomics* **8**, 15 (2007).
2. T. E. Dever, M. J. Glynias, W. C. Merrick, *Proc. Natl. Acad. Sci. U.S.A.* **84**, 1814 (1987).
3. D. Moazed, J. M. Robertson, H. F. Noller, *Nature* **334**, 362 (1988).
4. L. Holmberg, O. Nygård, *Biochemistry* **33**, 15159 (1994).
5. J. F. Eccleston, M. R. Webb, *J. Biol. Chem.* **257**, 5046 (1982).
6. H. Berchtold *et al.*, *Nature* **365**, 126 (1993).
7. M. Kjeldgaard, P. Nissen, S. Thirup, J. Nyborg, *Structure* **1**, 35 (1993).
8. E. Jacquet, A. Parmeggiani, *EMBO J.* **7**, 2861 (1988).
9. T. Pape, W. Wintermeyer, M. V. Rodnina, *EMBO J.* **17**, 7490 (1998).
10. J. R. Mesters, A. P. Potapov, J. M. de Graaf, B. Kraal, *J. Mol. Biol.* **242**, 644 (1994).
11. T. P. Hausner, J. Atmadja, K. H. Nierhaus, *Biochimie* **69**, 911 (1987).
12. H. R. Bourne, D. A. Sanders, F. McCormick, *Nature* **349**, 117 (1991).
13. D. Mohr, W. Wintermeyer, M. V. Rodnina, *Biochemistry* **41**, 12520 (2002).
14. L. Voegelé, G. J. Palm, J. R. Mesters, R. Hilgenfeld, *J. Biol. Chem.* **276**, 17149 (2001).
15. T. M. Schmeing *et al.*, *Science* **326**, 688 (2009).
16. J. Sengupta *et al.*, *J. Mol. Biol.* **382**, 179 (2008).
17. E. Villa *et al.*, *Proc. Natl. Acad. Sci. U.S.A.* **106**, 1063 (2009).
18. J. C. Schuette *et al.*, *EMBO J.* **28**, 755 (2009).
19. P. Nissen *et al.*, *Science* **270**, 1464 (1995).
20. M. Valle *et al.*, *EMBO J.* **21**, 3557 (2002).
21. D. J. Taylor *et al.*, *EMBO J.* **26**, 2421 (2007).
22. C. Knudsen, H. J. Wieden, M. V. Rodnina, *J. Biol. Chem.* **276**, 22183 (2001).
23. D. M. Blow, J. J. Birkoft, B. S. Hartley, *Nature* **221**, 337 (1969).
24. M. Selmer *et al.*, *Science* **313**, 1935 (2006).
25. N. Bilgin, M. Ehrenberg, *J. Mol. Biol.* **235**, 813 (1994).
26. F. Rambelli *et al.*, *Biochem. J.* **259**, 307 (1989).
27. J. M. Ogle *et al.*, *Science* **292**, 897 (2001).
28. R. Mittal, M. R. Ahmadian, R. S. Goody, A. Wittinghofer, *Science* **273**, 115 (1996).
29. K. Rittinger, P. A. Walker, J. F. Eccleston, S. J. Smerdon, S. J. Gamblin, *Nature* **389**, 758 (1997).
30. J. J. Tesmer, D. M. Berman, A. G. Gilman, S. R. Sprang, *Cell* **89**, 251 (1997).
31. M. Diaconu *et al.*, *Cell* **121**, 991 (2005).
32. H. J. Wieden, W. Wintermeyer, M. V. Rodnina, *J. Mol. Evol.* **52**, 129 (2001).
33. M. Remacha *et al.*, *Mol. Cell. Biol.* **15**, 4754 (1995).
34. M. V. Rodnina, R. Fricke, W. Wintermeyer, *Biochemistry* **33**, 12267 (1994).

35. We thank R. Green for reagents and D. de Sanctis at the European Synchrotron Radiation Facility for facilitating data collection. This work was supported by the Medical Research Council UK, the Wellcome Trust, the Agouron Institute, and the Louis-Jeanet Foundation. R.M.V. is supported by a Gates-Cambridge scholarship, and T.M.S. by the Human Frontier Science Program and Emmanuel College. V.R. is on the Scientific Advisory Board and holds stock options in Rib-X pharmaceuticals. Transfer of *Thermus thermophilus* ribosome strain T.th. HB8-MRC-MSAW1 requires a Materials Transfer Agreement with the MRC. Coordinates and structure factors have been deposited at the Protein Data Bank with accession codes 2xqd and 2xqc.

Supporting Online Material

www.sciencemag.org/cgi/content/full/330/6005/835/DC1
Materials and Methods

Figs. S1 to S4

Table S1

References

29 June 2010; accepted 3 September 2010

10.1126/science.1194460

Evolution of Yeast Noncoding RNAs Reveals an Alternative Mechanism for Widespread Intron Loss

Quinn M. Mitrovich,^{1,2*} Brian B. Tuch,^{1,3*†} Francisco M. De La Vega,³ Christine Guthrie,^{2‡} Alexander D. Johnson^{1,2‡}

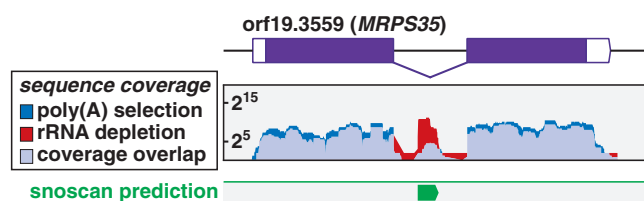
The evolutionary forces responsible for intron loss are unresolved. Whereas research has focused on protein-coding genes, here we analyze noncoding small nucleolar RNA (snoRNA) genes in which introns, rather than exons, are typically the functional elements. Within the yeast lineage exemplified by the human pathogen *Candida albicans*, we find—through deep RNA sequencing and genome-wide annotation of splice junctions—extreme compaction and loss of associated exons, but retention of snoRNAs within introns. In the *Saccharomyces* yeast lineage, however, we find it is the introns that have been lost through widespread degeneration of splicing signals. This intron loss, perhaps facilitated by innovations in snoRNA processing, is distinct from that observed in protein-coding genes with respect to both mechanism and evolutionary timing.

In eukaryotes, protein-coding genes are frequently interrupted by introns, which must be precisely removed from RNA transcripts by

the nuclear spliceosome (1). Over evolutionary time scales, the presence of introns is dynamic, with intron gain and loss rates varying substan-

tially across eukaryotic lineages (2–4). The mechanisms of intron gain and loss speak to questions about both the origins of introns and the markedly different intron-exon patterns observed across eukaryotes (5)—for example, whether spliceosomal introns arose within eukaryotes (“introns late”), within an ancestor of both prokaryotes and eukaryotes (“introns early”), or even before the emergence of protein-coding genes (“introns first”) (6). The last two hypotheses depend on the feasibility of comprehensive intron loss within both the prokaryotic and archaeal lineages, whose modern representatives lack spliceosomal introns. Within eukaryotes, the hemiascomycetous yeasts show substantial intron loss, with modern species like *Saccharomyces cerevisiae* and *Candida albicans* devoid of introns in >90% of their genes (7). A postulated mechanism for this loss is reverse transcription of spliced RNA, followed by homologous DNA recombination that replaces the intron-containing genomic sequence with the intronless copy (8). Previous studies of intron loss have focused on protein-coding genes, however, and are therefore likely to be biased toward mecha-

Fig. 1. Sequence library comparisons reveal noncoding RNAs. RNA sequence data are shown for *MRPS35*, a representative protein-coding gene that hosts a snoRNA within its intron. Nonadenylated RNAs, such as mature snoRNAs, are enriched in the rRNA-depleted library relative to the poly(A)-selected library. Sequence depth is represented on a log₂ axis. (Bottom track) One of 1706 lower-confidence snoRNA predictions generated using the snoscan algorithm (22).



¹Department of Microbiology and Immunology, University of California, San Francisco, San Francisco, CA 94143–2200, USA.

²Department of Biochemistry and Biophysics, University of California, San Francisco, San Francisco, CA 94143–2200, USA.

³Genetic Systems Division, Research and Development, Life Technologies, Foster City, CA 94404, USA.

*These authors contributed equally to this work.

†Present address: Genome Analysis Unit, Amgen, South San Francisco, CA 94080, USA.

‡To whom correspondence should be addressed. E-mail: christineguthrie@gmail.com (C.G.); ajohnson@cgl.ucsf.edu (A.D.J.)



Supporting Online Material for
The Mechanism for Activation of GTP Hydrolysis on the Ribosome

Rebecca M. Voorhees, T. Martin Schmeing, Ann C. Kelley, V. Ramakrishnan*

*To whom correspondence should be addressed. E-mail: ramak@mrc-lmb.cam.ac.uk

Published 5 November 2010, *Science* **330**, 835 (2010)
DOI: 10.1126/science.1194460

This PDF file includes:

Materials and Methods
Figs. S1 to S4
Table S1
References

Materials and Methods

Ribosomes from *Thermus thermophilus* harboring a C-terminal truncation of protein L9(1) were purified as previously described(2) from cells grown at the Bioexpression and Fermentation Facility at the University of Georgia. mRNA with the sequence 5'GGCAAGGAGGUAAAAAUGUUCUGGAAA was purchased from Dharmcon (Thermo Scientific). Trp-tRNA^{Trp} was prepared as described (3).

Complexes of trp-tRNA^{Trp}-GDPCP-70S ribosome were prepared and purified by Ni-NTA affinity purification as described (3) with the exception that the antibiotic paromomycin was included in the reaction mixture to increase sample yield. The trp-tRNA^{Trp} used in this study contained a G24A mutation, which increased the reproducibility of crystal growth. On cognate mRNA, it is known that this tRNA behaves identically to wild type trp-tRNA^{Trp}(4) and crystal structures of G24A and tRNA^{Trp} and bound to the ribosome on the cognate codon are extremely similar (3).

Crystals were grown as described(5) by vapor diffusion in sitting drop trays by addition of 3 μ L reservoir (100 mM MES pH 6.3, 60-100 mM KCl, 50 mM sucrose, 1% glycerol, and 5.3% (w/v) PEG20K) to 3 μ L of the 70S-TC sample, and cryo-protected stepwise to a final solution of 100 mM MES pH 6.3, 100 mM KCl, 50 mM sucrose, 1.1% glycerol, 6.0% (w/v) PEG20K, 15 mM MgOAc₂, and 30% (w/v) PEG400 before being frozen by plunging into liquid nitrogen.

Data was collected at beamline ID 14-4 of the European Synchrotron Light Source(6), and integrated and scaled using XDS(7). These crystals are in space group P2₁, with unit cell dimensions a=197.6 b=274.9 c=282.5, β =91.8. This crystal form is related to our previous crystals (5) (3), which were also in P2₁, but the length of the a axis is doubled in the previous form. The two forms are related by a small translation of the ribosome, which converts the non-crystallographic symmetry in the larger unit cell into crystallographic symmetry, leading to only one ribosome molecule in this smaller asymmetric unit.

The structure was determined by molecular replacement in CNS(8), using a ligand-free ribosome as the search model. Iterative rounds of model building and refinement were carried out in coot(9) and CNS(8) as previously described(5). To avoid contamination of R_{free} , the R_{free} set was inherited from our previous data with the conversion $h_{\text{new}}=l_{\text{old}}/2$, $k_{\text{new}}=-k_{\text{old}}$, $l_{\text{new}}=h_{\text{old}}$ to account for the change in unit cell. All figures were made in Pymol(10).

Supplemental Figures

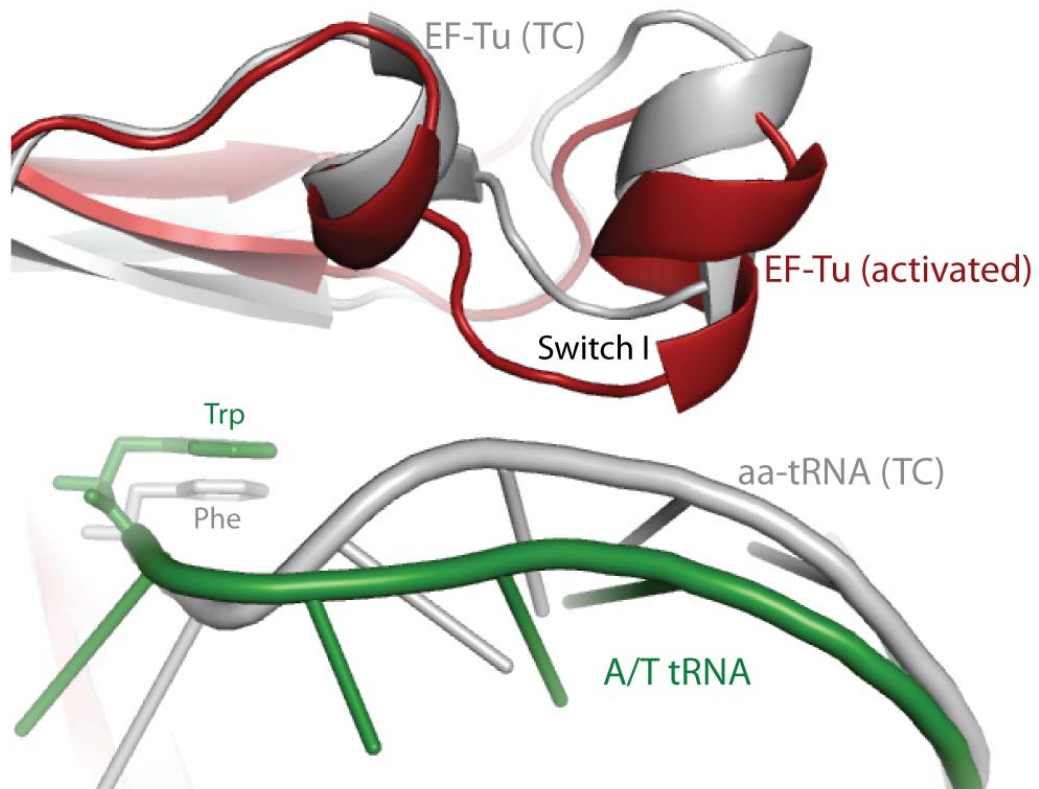


fig s1. Binding the ribosome induces a distortion in the 3' end of the aminoacyl-tRNA (green—activated structure, grey—isolated TC) that disrupts interactions between the Switch I loop of EF-Tu (red—activated, grey—TC) and the tRNA backbone.

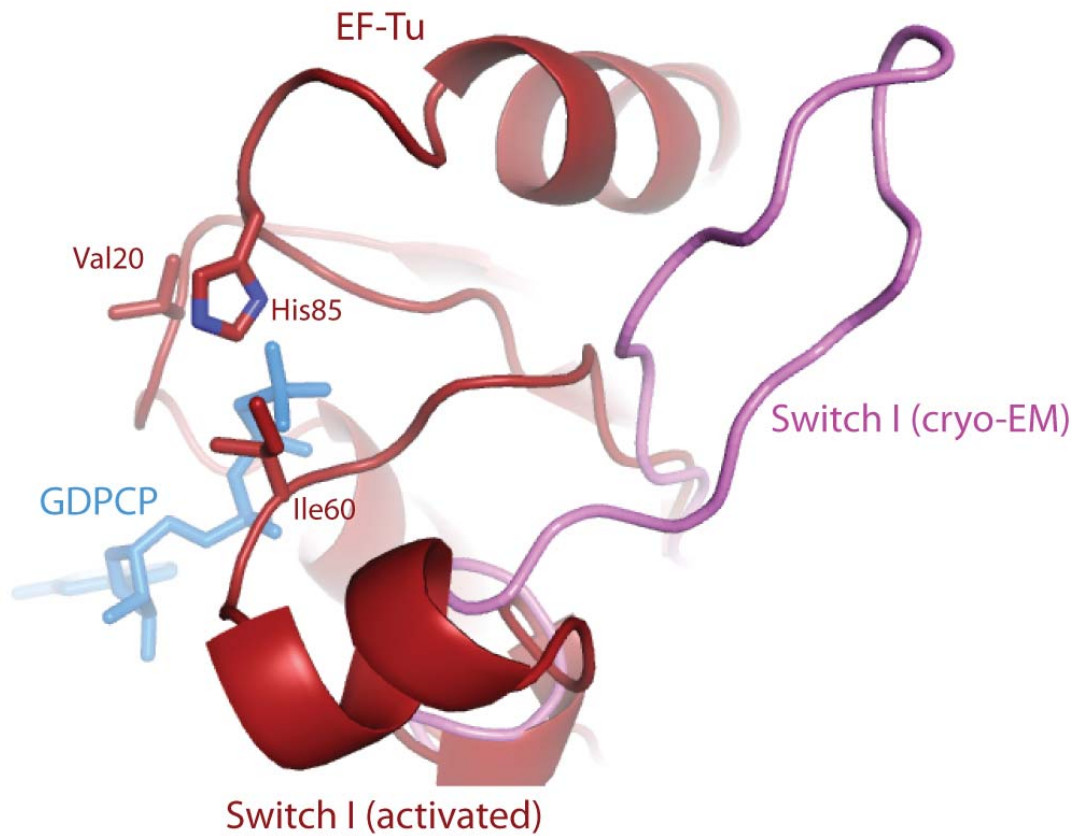


fig s2. In the activated structure of EF-Tu bound to the ribosome, the Switch I loop (red) is in a well ordered and located in the GTPase center. We see no evidence that a disordered or radically remodeled Switch I (pink)(11) is required for GTPase activation and hydrolysis on the ribosome.

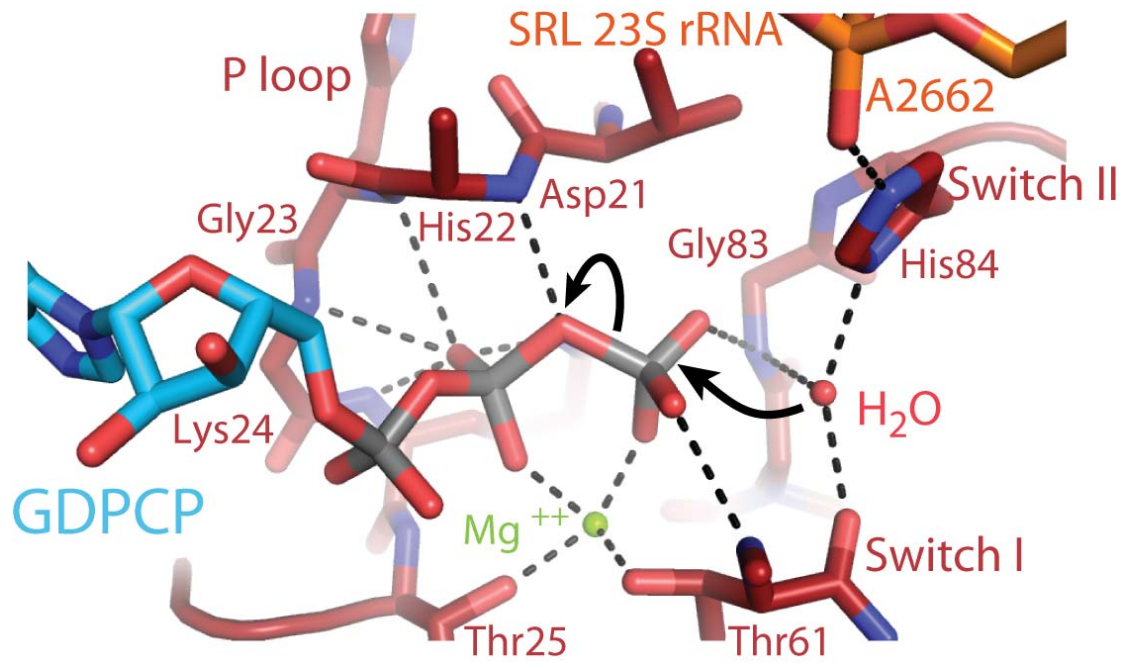


fig s3. Several interactions between EF-Tu and the GTP stabilize the β and γ phosphates that are important for GTP hydrolysis. Additionally, several interactions between the Switch I residue Thr61 and the γ phosphate explain how release of Pi results in the disordering of Switch I.

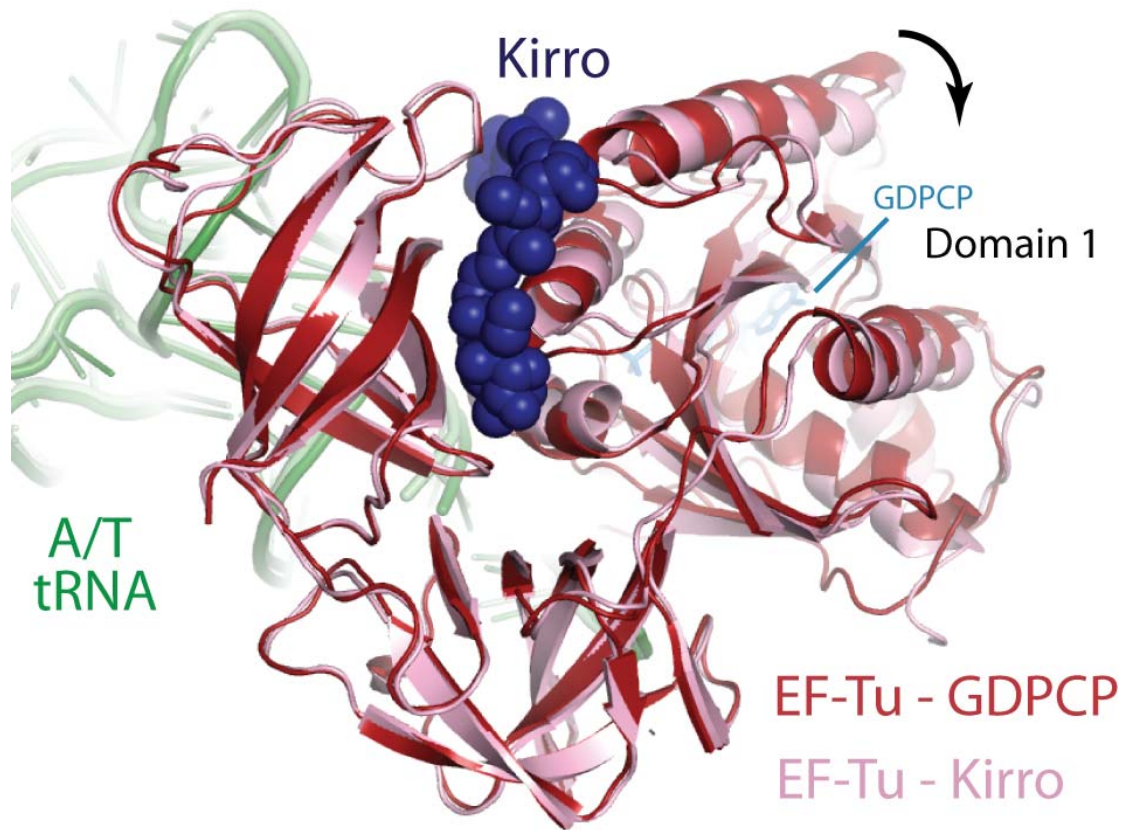


fig s4. A small rotation in the G-domain of EF-Tu relative to domains 2 and 3 is observed between the GDPCP (red) and kirromycin (pink) stabilized structures bound to the ribosome.

Table s1. Summary of crystallographic data and refinement

Data collection	70S-TC-GDPCP (merged from 3 crystals)
Space Group	P2 ₁
Cell dimensions	
<i>a</i> , <i>b</i> , <i>c</i> (Å)	<i>a</i> =197.6 <i>b</i> =274.9 <i>c</i> =282.5
α , β , γ (°)	α =90.0 β =91.8 γ =90.0
Resolution (Å)	50-3.1 (3.2-3.1) * [†]
R _{sym} (%)	22.8 (126.3)
<i>I</i> / σ <i>I</i>	6.98 (1.16) *
Completeness (%)	98.8(89.6)
Redundancy	5.2 (4.3)
Refinement	
Resolution (Å)	50.0-3.1 [†]
No. unique reflections	537024
<i>R</i> _{work} / <i>R</i> _{free}	23.1/26.8
No. atoms	
RNA	102,537
Protein	50,602
<i>B</i> -factors	
RNA	83
Protein	87
R.m.s deviations	
Bond lengths (Å)	0.007
Bond angles (°)	1.2

* *I*/ σ *I* = 1.88 at 3.2 Å resolution (using a bin from 3.4-3.2 Å resolution)

[†] *R*_{work}/*R*_{free} = 33.2/35.4 for data from 3.2-3.1 Å resolution

References

1. Y. G. Gao *et al.*, *Science* **326**, 694 (2009).
2. M. Selmer *et al.*, *Science* **313**, 1935 (2006).
3. T. M. Schmeing, Voorhees, R.M., Kelley, A.C., and V. Ramakrishnan, *Submitted* (2010).
4. L. Cochella, R. Green, *Science* **308**, 1178 (2005).
5. T. M. Schmeing *et al.*, *Science* **326**, 688 (2009).
6. A. A. McCarthy *et al.*, *J Synchrotron Radiat* **16**, 803 (2009).
7. W. Kabsch, *J. Appl. Cryst.* **26**, 795 (1993).
8. A. T. Brünger *et al.*, *Acta Crystallogr D Biol Crystallogr* **54**, 905 (1998).
9. P. Emsley, K. Cowtan, *Acta Crystallogr D Biol Crystallogr* **60**, 2126 (2004).
10. W. L. DeLano, <http://www.pymol.org> (2006).
11. E. Villa *et al.*, *Proc Natl Acad Sci U S A* **106**, 1063 (2009).